VOL. 10, NO. 12, JULY 2015 ISSN 1819-6608
ARPN Journal of Engineering and Applied Sciences

www.arpnjournals.com

FINITE ELEMENT ANALYSIS OF UNSTEADY MHD FREE CONVECTION FLOW PAST AN INFINITE VERTICAL PLATE WITH SORET, DUFOUR, THERMAL RADIATION AND HEAT SOURCE

J. Anand Rao[1], P. Ramesh Babu[2] and R. Srinivasa Raju[3]
[1]Department of Mathematics, University College of Science, Osmania University, Hyderabad, Telangana State, India
[2]Department of Mathematics, Sri Kottam Tulasi Reddy Memorial College of Engineering, Kondair Village, Itikyal Mandal, Mahaboob Nagar (Dt), Telangana State, India
[3]Department of Mathematics, GITAM University, Hyderabad Campus, Rudraram, Telangana State, India
E-Mail: ramesh.patkar@yahoo.in

ABSTRACT

A study has been carried out to analyze the combined effects of Soret (thermal-diffusion) and Dufour (diffusion-thermo) on an unsteady magnetohydro dynamic free convection flow past an infinite vertical plate in a porous medium in presence of thermal radiation and heat source. A uniform magnetic field acts perpendicular to the porous surface. Energy equation takes into account of viscous dissipation, thermal radiation and Dufour effects. The governing differential equations are transformed into a set of non-linear coupled partial differential equations and solved using similarity analysis with numerical technique using appropriate boundary conditions for various physical parameters. The dimensionless governing equations are solved numerically using Galerkin finite element method. Favorable comparisons with previously published work on various special cases of the problem are obtained. The effects of various physical parameters on the dimensionless velocity, temperature and concentration profiles are presented graphically. In addition, the local values of the Skin-friction coefficient, Nusselt number and Sherwood number are also shown in tabular form.

Keywords: soret and dufour, thermal radiation, heat source, MHD, galerkin finite element method.

1. INTRODUCTION

Convection flows in porous media have gained significant attention in the recent years because of their importance in engineering applications such as geothermal systems, solid matrix heat exchangers, thermal insulations, oil extraction and store of nuclear waste materials. These can also be applied to underground coal gasification, ground water hydrology, wall cooled catalytic reactors, energy efficient drying processes and natural convection in earth's crust. The unsteady MHD transient free convection flow of an incompressible viscous electrically conducting fluid between two infinite vertical parallel porous plates with variable temperature and mass diffusion has been studied by Rajput and Sahu (2011), under the assumption that the induced magnetic field is negligible. Applied magnetic field is fixed relative to the fluid and plates. The Laplace transform method has been used to find the solutions for the velocity, temperature and concentration profiles. Anand Rao and Srinivasa Raju (2010) investigated applied magnetic field on transient free convective flow of an incompressible viscous dissipative fluid in a vertical channel. El-Amin (2001) considered the MHD free convection and mass transfer flow in a micropolar fluid over a stationary vertical plate with constant suction. Chaudhary and Sharma (2006) considered combined heat and mass transfer by laminar mixed convection flow from a vertical surface with induced magnetic field. Hydromagnetic unsteady mixed convection and mass transfer flow past a vertical porous plate immersed in a porous medium was investigated by Sharma and Chaudhary (2008). Kandasamy *et al.* (2005) discussed heat and mass transfer effect along a wedge with heat source and concentration in the presence of suction/injection taking into account the chemical reaction of first order.

When technological processes take place at higher temperatures thermal radiation heat transfer has become very important and its effects cannot be neglected. The effect of radiation on MHD flow, heat and mass transfer become more important industrially. Many processes in engineering areas occur at high temperature and knowledge of radiation heat transfer becomes a very important for the design of the pertinent equipment. The quality of the final product depends to a great extent on the heat controlling factors, and the knowledge of radiative heat transfer in the system can lead to a desired product with sought qualities. The effects of variable viscosity and chemical reaction effects on flow, heat and mass transfer characteristics in a viscous fluid over a porous wedge in the presence of heat radiation studied by Kandasamy *et al.* (2007). The wall of the wedge is embedded in a uniform Darcian porous medium in order to allow for possible fluid wall suction or injection. The governing boundary layer equations are written into a dimensionless form by similarity transformations. The transformed coupled nonlinear ordinary differential equations are solved numerically by using the R. K. Gill and shooting methods. The effects of thermal radiation on unsteady free

convection flow past an exponentially accelerated infinite isothermal vertical plate with mass transfer in the presence of magnetic field by Rajesh and Vijaya Kumar Varma (2009). The fluid considered here is a gray, absorbing/emitting radiation but a non-scattering medium. The governing equations are solved in closed form by the Laplace transform technique. The radiation effect on unsteady heat and mass transfer flow of a chemically reacting fluid past a semi-infinite vertical plate with viscous dissipation studied by Srinivasa Rao and Anand Babu (2010). Unsteady MHD flow, radiation and mass transfer of a viscous incompressible conducting fluid past on impulsively started infinite vertical porous plate with variable temperature in the presence of homogeneous chemical reaction is studied by Anand Rao *et al.* (2012). The governing equations are solved by using the finite element method. Radiation effects on MHD flow through porous media past an impulsively started vertical oscillating plate with variable mass diffusion is studied by Rajput and Surendra Kumar (2012). The fluid considered is gray, absorbing-emitting radiation but a non-scattering medium. The governing equations involved in the present analysis are solved by the Laplace transform technique. Vijay Kumar *et al.* (2013) investigated the effects of the heat source, chemical reaction and radiation absorption on unsteady MHD flow with heat and mass transfer of an incompressible, viscous, electrically conducting fluid past an infinite vertical moving plate with constant temperature in the presence of transverse applied magnetic field. An exact solution for the flow problem has been obtained by solving the governing equations using Laplace transform technique. Influence of viscous dissipation and radiation on unsteady MHD free convection flow past an infinite heated vertical plate in a porous medium with time-dependent suction studied by Israel-Cookey *et al.* (2003).

But in the above mentioned studies, Dufour and Soret terms have been neglected from the energy and concentration equations respectively. It has been found that energy flux can be generated not only by temperature gradient but also by concentration gradient as well. The energy flux caused by concentration gradient is called Dufour effect and the same by temperature gradient is called the Soret effect. These effects are very significant when the temperature and concentration gradient are very high. Mohammad Ali and Mohammad Shah Alam (2014) discussed the effect of Soret and Hall current due to heat generation on coupled heat and mass transfer by magnetohydrodynamic free convection over a permeable vertical stretching sheet. The governing boundary layer equations are formulated and transformed into a set of similarity equations using dimensionless similarity variables. The governing fundamental set of a system of non-linear locally similar ordinary differential equations are solved numerically by Runge-Kutta fourth-fifth order integration scheme along with shooting technique. The effects of Hall currents, Soret and Dufour on an unsteady magnetohydrodynamic flow and heat transfer along a porous flat plate with mass transfer studied by Anand Rao and Srinivasa Raju (2011). Postelnicu (2004) studied simultaneous heat and mass transfer by natural convection from a vertical plate embedded in electrically conducting fluid saturated porous medium, using Darcy-Boussinesq's model including Soret, and Dufour effects. Afify (2009) carried out an analysis to study free convective heat and mass transfer of an incompressible, electrically conducting fluid over a stretching sheet in the presence of suction and injection with thermal-diffusion and diffusion-thermo effects. Alam *et al*. (2006) studied numerically the Dufour and Soret effects on combined free-forced convection and mass transfer flow past a semi-infinite vertical plate under the influence of transversely applied magnetic field. Mansour *et al.* (2008) investigated the effects of chemical reaction, thermal stratification, Soret and Dufour numbers on MHD free convective heat and mass transfer of a viscous, incompressible and electrically conducting fluid over a vertical stretching surface embedded in a saturated porous medium. Osalusi *et al*. (2008) investigated thermo diffusion and diffusion-thermo effects on combined heat and mass transfer of a steady hydromagnetic convective and slip flow due to a rotating disk in the presence of viscous dissipation and Ohmic heating. The effects of thermal radiation and Heat source on an unsteady MHD free convection flow past an infinite vertical plate with thermal-diffusion and diffusion-thermo discussed by Srinivasa Raju *et al*. (2013).

In spite of all these studies, the Dufour and Soret effects on unsteady MHD free convective heat and mass transfer past an infinite vertical plate embedded in a porous medium in the presence of thermal radiation and heat source has received little attention. Hence, the purpose of this paper is to extend Israel-Cookey *et al.* (2003) to study the more general problem which includes Thermal radiation, Heat source, Soret and Dufour on unsteady MHD free convective flow past an infinite vertical plate. The momentum, thermal, and solutal boundary layer governing equations are transformed into a set of partial differential equations and then solved using Galerkin finite element method. The effects of various governing parameters on the velocity, temperature, and concentration profiles as well as the local skin-friction coefficient, local Nusselt number and local Sherwood number are presented graphically and in tabular form. The rest of the paper is structured as follows. In Section 2, we formulate the problem in Section 3, we give the method of solution. Our results are presented and discussed in Section 4 and in Section 5, we present some brief conclusions.

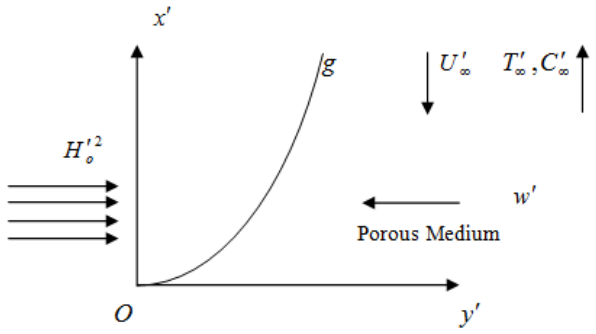

Figure-1. The physical model and coordinate system of the problem.

FORMULATION OF THE PROBLEM

We consider the unsteady flow of an incompressible viscous, radiating hydromagnetic fluid past an infinite porous heated vertical plate with time-dependent suction in an optically thin environment. The physical model and the coordinate system are shown in Figure-1. The $x'-$ axis is taken along the vertical infinite porous plate in the upward direction and the $y'-$ axis normal to the plate. At time $t'=0$, the plate is maintained at a temperature T'_w, which is high enough to initiate radiative heat transfer. A constant magnetic field H'^2_o is maintained in the y' direction and the plate moves uniformly along the positive $x'-$ direction with velocity U_0. Under Boussinesq's approximation the flow is governed by the following equations:

Equation of continuity

$$\frac{\partial w'}{\partial y'}=0 \tag{1}$$

Momentum Equation

$$\frac{\partial u'}{\partial t'}+w'\frac{\partial u'}{\partial y'}=\nu\frac{\partial^2 u'}{\partial y'^2}+\frac{\partial U'}{\partial t'}-\left(\frac{\mu^2\sigma_C H'^2_0}{\rho}+\frac{\nu}{k}\right)(u'-U')+g\beta\left(T'-T'_\infty\right)+g\beta^*\left(C'-C'_\infty\right) \tag{2}$$

Energy equation

$$\frac{\partial T'}{\partial t'}+w'\frac{\partial T'}{\partial y'}=\frac{k}{\rho\, c_P}\left(\frac{\partial^2 T'}{\partial y'^2}-\nabla q'_{z'}\right)-\frac{Q_o}{\rho c_P}(T'-T'_\infty)+\frac{D_m k_T}{c_S c_P}\frac{\partial^2 C'}{\partial y'^2} \tag{3}$$

Equation of radiative heat flux

$$\frac{\partial^2 q'_{z'}}{\partial y'^2}-3\alpha^2 q'_{z'}-16\alpha\,\sigma\, T_\infty^{\,3}\frac{\partial T'}{\partial y'}=0 \tag{4}$$

Species diffusion equation

$$\frac{\partial C'}{\partial t'}+w'\frac{\partial C'}{\partial y'}=D\frac{\partial^2 C'}{\partial y'^2}+\frac{D_m k_T}{T_m}\frac{\partial^2 T'}{\partial y'^2} \tag{5}$$

The corresponding boundary conditions are

$$\begin{aligned} &t'\le 0:\ \ u'=0,\ T'=T'_\infty,\ C'=C'_\infty\ \ for\ all\ \ y' \\ &t'>0:\begin{cases} u'=0,\ T'=T'_w,\ C'=C'_w\ \ at\ \ y'=0 \\ u'=U'(t')=w'_0\left(1+\varepsilon\, e^{i\omega' t'}\right),\ T'=T'_\infty,\ C'=C'_\infty\ \ as\ \ y'\to\infty \end{cases} \end{aligned} \tag{6}$$

Since the medium is optically thin with relatively low density and $\alpha<<1$ the radiative heat flux given by equation (4) in the spirit of Cogley *et al.* (1968) becomes

$$\frac{\partial q'_{z'}}{\partial y'}=4\alpha^2\left(T'-T'_\infty\right) \tag{7}$$

Where $\alpha^2=\int_0^\infty \delta\lambda\frac{\partial B}{\partial T'}$ (8)

Here λ is a frequency.

Further, from equation (1) it is clear that w' is a constant or a function of time only and so we assume

$$w'=-w'_0\left(1+\varepsilon A e^{i\omega' t'}\right) \tag{9}$$

Such that $\varepsilon A<<1$, and the negative sign indicates that the suction velocity is towards the plate. In view of equations (4), (8) and (9), equations (2), (3) and (5) become

Momentum equation

$$\frac{1}{4}\frac{\partial u}{\partial t}-\left(1+\varepsilon A\, e^{i\omega t}\right)\frac{\partial u}{\partial y}=\frac{1}{4}\frac{\partial U}{\partial t}+\frac{\partial^2 u}{\partial y^2}-(M^2+\chi^2)(u-U)+Gr\theta+GcC \tag{10}$$

Energy equation

$$\frac{1}{4}(\mathrm{Pr})\frac{\partial \theta}{\partial t}-(\mathrm{Pr})\left(1+\varepsilon A\, e^{i\omega t}\right)\frac{\partial \theta}{\partial y}=\left(\frac{\partial^2}{\partial y^2}-R^2\right)\theta-(\mathrm{Pr})(S)\theta+(\mathrm{Pr})(Du)\left(\frac{\partial^2 C}{\partial y^2}\right) \tag{11}$$

Species diffusion equation

$$\frac{1}{4}(Sc)\frac{\partial C}{\partial t}-(Sc)\left(1+\varepsilon A\, e^{i\omega t}\right)\frac{\partial C}{\partial y}=\frac{\partial^2 C}{\partial y^2}+(Sc)(Sr)\left(\frac{\partial^2 \theta}{\partial y^2}\right) \tag{12}$$

Where we have used the following dimensionless variables:

$$\left.\begin{aligned}
&t=\frac{w_0'^2 t'}{4\nu},\ y=\frac{w_0' y'}{\nu},\ u=\frac{u'}{U_0},\ w=\frac{4\nu\omega'}{w_0'^2},\ U=\frac{U'}{U_0},\ \theta=\frac{T'-T_\infty'}{T_w'-T_\infty'},\ \chi^2=\frac{\nu^2}{k w_0'^2},\ \mathrm{Pr}=\frac{\mu\, c_p}{k},\\
&Gr=\frac{g\beta\ \nu\left(T_w'-T_\infty'\right)}{U_0 w_0'^2},\quad Gc=\frac{g\beta^*\ \nu\left(C_w'-C_\infty'\right)}{U_0 w_0'^2},\ R^2=\frac{4\alpha^2}{\rho\, c_P k w_0'^2}(T_w'-T_\infty'),\ S=\frac{\nu Q_o}{\rho c_p w_0'^2},\\
&M^2=\frac{\mu^2\sigma_C H_0'^2}{\rho w_0'^2},\ Sr=\frac{D_m k_T\left(T_w'-T_\infty'\right)}{w_o T_m\left(C_w'-C_\infty'\right)},\ Du=\frac{D_m k_T\left(C_w'-C_\infty'\right)}{c_S c_P\left(T_w'-T_\infty'\right)},\ Sc=\frac{w_o}{D},\ \phi=\frac{\left(C'-C_\infty'\right)}{\left(C_w'-C_\infty'\right)}
\end{aligned}\right\} \tag{13}$$

Equations (10), (11) and (12) are now subject to the boundary conditions

$$\left.\begin{aligned}
&t\le 0:\ u=0,\quad \theta=0,\ \phi=0\quad for\ all\ y\\
&t>0:\begin{cases}u=0,\quad \theta=1,\phi=1\ \ on\ \ y=0\\ u\to 1+\varepsilon\, e^{i\omega t},\ \theta\to 0,\phi\to 0\ as\ \ y\to\infty\end{cases}
\end{aligned}\right\} \tag{14}$$

The mathematical statement of the problem is now complete and embodies the solution of equations (10), (11) and (12) subject to boundary conditions (14). The Skin-friction, Nusselt number and Sherwood number are important physical parameters for this type of boundary layer flow.

The Skin-friction at the plate, which in the non-dimensional form is given by

$$\tau=\frac{\tau_w'}{\rho U_o \nu}=\left(\frac{\partial u}{\partial y}\right)_{y=0} \tag{15}$$

The rate of heat transfer coefficient, which in the non-dimensional form in terms of the Nusselt number is given by

$$Nu=-x\frac{\left(\frac{\partial T'}{\partial y'}\right)_{y'=0}}{T_w'-T_\infty'}\ \Rightarrow Nu\,\mathrm{Re}_x^{-1}=-\left(\frac{\partial\theta}{\partial y}\right)_{y=0} \tag{16}$$

The rate of mass transfer coefficient, which in the non-dimensional form in terms of the Sherwood number, is given by

$$Sh=-x\frac{\left(\frac{\partial C'}{\partial y'}\right)_{y'=0}}{C_w'-C_\infty'}\ \Rightarrow Sh\,\mathrm{Re}_x^{-1}=-\left(\frac{\partial C}{\partial y}\right)_{y=0} \tag{17}$$

Where $\mathrm{Re}=\frac{U_o x}{\nu}$ is the local Reynolds number.

3. NUMERICAL SOLUTION BY FINITE ELEMENT METHOD

By applying Galerkin finite element method for equation (10) over the element (e), $\left(y_j \le y \le y_k\right)$ is:

$$\int_{y_j}^{y_k}\left\{N^{(e)T}\left[4\frac{\partial^2 u^{(e)}}{\partial y^2}-\frac{\partial u^{(e)}}{\partial t}+4B\frac{\partial u^{(e)}}{\partial y}-Du^{(e)}+P\right]\right\}dy=0 \tag{18}$$

Where $P=\frac{\partial U}{\partial t}+4(Gr)\theta+4(Gc)C+DU$, $B=1+\varepsilon Ae^{i\omega t}$, $D=4(M^2+\chi^2)$;

Integrating the first term in equation (18) by parts one obtains

$$4N^{(e)T}\left\{\frac{\partial u^{(e)}}{\partial y}\right\}_{y_j}^{y_k}-\int_{y_j}^{y_k}\left\{4\frac{\partial N^{(e)T}}{\partial y}\frac{\partial u^{(e)}}{\partial y}+N^{(e)T}\left(\frac{\partial u^{(e)}}{\partial t}-4B\frac{\partial u^{(e)}}{\partial y}+Du^{(e)}-P\right)\right\}dy=0 \tag{19}$$

Neglecting the first term in equation (19), one gets:

$$\int_{y_j}^{y_k}\left\{4\frac{\partial N^{(e)T}}{\partial y}\frac{\partial u^{(e)}}{\partial y}+N^{(e)T}\left(\frac{\partial u^{(e)}}{\partial t}-4B\frac{\partial u^{(e)}}{\partial y}+Du^{(e)}-P\right)\right\}dy=0$$

Let $u^{(e)}=N^{(e)}\phi^{(e)}$ be the linear piecewise approximation solution over the element (e) ($y_j \le y \le y_k$) where $N^{(e)}=\begin{bmatrix}N_j & N_k\end{bmatrix}$, $\phi^{(e)}=\begin{bmatrix}u_j & u_k\end{bmatrix}^T$ and $N_j=\frac{y_k-y}{y_k-y_j}$, $N_k=\frac{y-y_j}{y_k-y_j}$ are the basis functions. One obtains:

$$4\int_{y_j}^{y_k}\left\{\begin{bmatrix}N_j' N_j' & N_j' N_k' \\ N_j' N_k' & N_k' N_k'\end{bmatrix}\begin{bmatrix}u_j \\ u_k\end{bmatrix}\right\}dy+\int_{y_j}^{y_k}\left\{\begin{bmatrix}N_j N_j & N_j N_k \\ N_j N_k & N_k N_k\end{bmatrix}\begin{bmatrix}\dot{u}_j \\ \dot{u}_k\end{bmatrix}\right\}dy-4B\int_{y_j}^{y_k}\left\{\begin{bmatrix}N_j N_j' & N_j N_k' \\ N_j' N_k & N_k' N_k\end{bmatrix}\begin{bmatrix}u_j \\ u_k\end{bmatrix}\right\}dy$$

$$+D\int_{y_j}^{y_k}\left\{\begin{bmatrix}N_j N_j & N_j N_k \\ N_j N_k & N_k N_k\end{bmatrix}\begin{bmatrix}u_j \\ u_k\end{bmatrix}\right\}dy=P\int_{y_j}^{y_k}\begin{bmatrix}N_j \\ N_k\end{bmatrix}dy$$

Simplifying we get

$$\frac{4}{l^{(e)^2}}\begin{bmatrix}1 & -1 \\ -1 & 1\end{bmatrix}\begin{bmatrix}u_j \\ u_k\end{bmatrix}+\frac{1}{6}\begin{bmatrix}2 & 1 \\ 1 & 2\end{bmatrix}\begin{bmatrix}\dot{u}_j \\ \dot{u}_k\end{bmatrix}-\frac{4B}{2l^{(e)}}\begin{bmatrix}-1 & 1 \\ -1 & 1\end{bmatrix}\begin{bmatrix}u_j \\ u_k\end{bmatrix}+\frac{D}{6}\begin{bmatrix}2 & 1 \\ 1 & 2\end{bmatrix}\begin{bmatrix}u_j \\ u_k\end{bmatrix}=\frac{P}{2}\begin{bmatrix}1 \\ 1\end{bmatrix}$$

Where prime and dot are denotes differentiation with respect to y and time t respectively. Assembling the element equations for two consecutive elements $\left(y_{i-1} \le y \le y_i\right)$and $\left(y_i \le y \le y_{i+1}\right)$ following is obtained:

$$\frac{4}{l^{(e)^2}}\begin{bmatrix}1 & -1 & 0\\ -1 & 2 & -1\\ 0 & -1 & 1\end{bmatrix}\begin{bmatrix}u_{i-1}\\ u_i\\ u_{i+1}\end{bmatrix}+\frac{1}{6}\begin{bmatrix}2 & 1 & 0\\ 1 & 4 & 1\\ 0 & 1 & 2\end{bmatrix}\begin{bmatrix}\dot{u}_{i-1}\\ \dot{u}_i\\ \dot{u}_{i+1}\end{bmatrix}-\frac{4B}{2l^{(e)}}\begin{bmatrix}-1 & 1 & 0\\ -1 & 0 & 1\\ 0 & -1 & 1\end{bmatrix}\begin{bmatrix}u_{i-1}\\ u_i\\ u_{i+1}\end{bmatrix}+$$
$$\frac{D}{6}\begin{bmatrix}2 & 1 & 0\\ 1 & 4 & 1\\ 0 & 1 & 2\end{bmatrix}\begin{bmatrix}u_{i-1}\\ u_i\\ u_{i+1}\end{bmatrix}=\frac{P}{2}\begin{bmatrix}1\\ 2\\ 1\end{bmatrix} \quad (20)$$

Now put row corresponding to the node i to zero, from equation (20) the difference schemes with $l^{(e)}=h$ is:

$$\frac{4}{h^2}\left[-u_{i-1}+2u_i-u_{i+1}\right]+\frac{1}{6}\left[\dot{u}_{i-1}+4\dot{u}_i+\dot{u}_{i+1}\right]-\frac{4B}{2h}\left[-u_{i-1}+u_{i+1}\right]+\frac{D}{6}\left[u_{i-1}+4u_i+u_{i+1}\right]=P \quad (21)$$

Applying the trapezoidal rule, following system of equations in Crank-Nicholson method are obtained:

$$A_1u_{i-1}^{n+1}+A_2u_i^{n+1}+A_3u_{i+1}^{n+1}=A_4u_{i-1}^{n}+A_5u_i^{n}+A_6u_{i+1}^{n}+P^* \quad (22)$$

Now from equations (11) and (12) following equations are obtained:

$$B_1\theta_{i-1}^{n+1}+B_2\theta_i^{n+1}+B_3\theta_{i+1}^{n+1}=B_4\theta_{i-1}^{n}+B_5\theta_i^{n}+B_6\theta_{i+1}^{n}+Q^* \quad (23)$$

$$C_1C_{i-1}^{n+1}+C_2C_i^{n+1}+C_3C_{i+1}^{n+1}=C_4C_{i-1}^{n}+C_5C_i^{n}+C_6C_{i+1}^{n}+R^* \quad (24)$$

Where

$A_1=2-12Brh-Dk-24r,\ A_2=8+4Dk+48r,$
$A_3=2+12Brh+Dk-24r,$
$A_4=2-12Brh-Dk+24r,\ A_5=8-4Dk-48r,$
$A_6=2+12Brh+Dk+24r,$
$B_1=2(\mathrm{Pr})-12(\mathrm{Pr})Brh-4R^2k-24r-4(\mathrm{Pr})Sk,$
$B_2=8(\mathrm{Pr})+48r+16R^2k+16(\mathrm{Pr})Sk,$
$B_3=2(\mathrm{Pr})+12(\mathrm{Pr})Brh+4R^2k-24r+4(\mathrm{Pr})Sk,$
$B_4=2(\mathrm{Pr})-12(\mathrm{Pr})Brh-4R^2k+24r-4(\mathrm{Pr})Sk,$
$B_5=8(\mathrm{Pr})-48r-16R^2k-16(\mathrm{Pr})Sk,$
$B_6=2(\mathrm{Pr})+12(\mathrm{Pr})Brh-4R^2k+24r-4(\mathrm{Pr})Sk,$
$C_1=2(Sc)-12(\mathrm{Pr})Brh-24r,\ C_2=8(Sc)+48r,$
$C_3=2(Sc)+12(Sc)Brh-24r,$
$C_4=2(Sc)-12(Sc)Brh+24r,\ C_5=8(Sc)-48r,$
$C_6=2(Sc)+12(Sc)Brh+24r,$
$P^*=12Pk=12k\left(\frac{\partial U}{\partial t}+4(Gr)\theta+DU\right),$
$Q^*=12Qk=48(\mathrm{Pr})k(Du)\left(\frac{\partial^2 C}{\partial y^2}\right),$
$R^{**}=12R^*k=48(Sc)(Sr)k\left(\frac{\partial^2\theta}{\partial y^2}\right);$

Here r= $\frac{k}{h^2}$ and h, k are mesh sizes along y-direction and time-direction respectively. Index i refers to space and j refers to the time. In the equations (22), (23) and (24), taking $i=1(1)n$ and using boundary conditions (14), then the following system of equations are obtained:

$$A_iX_i=B_i \quad for\ i=1(1)n \quad (25)$$

where $A_i^{'}$s are matrices of order n and $X_i, B_i^{'}$s are column matrices having n-components. The solutions of above system of equations are obtained by using Thomas algorithm for velocity, temperature and concentration. Also, numerical solutions for these equations are obtained by MATLAB-programme. In order to prove the convergence and stability of Galerkin finite element method, the same MATLAB-programme was run with smaller values of h and k no significant change was observed in the values of u, θ and C. Hence the Galerkin finite element method is stable and convergent.

RESULTS AND DISCUSSIONS

In the previous sections, we have formulated and solved the problem of an unsteady MHD free convection flow past an infinite heated vertical plate in a porous medium with thermal-diffusion, diffusion-thermo, radiation and heat source. By invoking, the optically thin differential approximation for the radiative heat flux in the energy equation. In the numerical computation, the Prandtl number ($\Pr = 0.71$) which corresponds to air and various values of the material parameters are used. In addition, the boundary condition $y \to \infty$ is approximated by $y_{\max} = 4$, which is sufficiently large for the velocity to approach the relevant stream velocity. The temperature and the species concentration are coupled to the velocity via Grashof number (Gr) and Modified Grashof number (Gc) as seen in equation (10). For various values of Grashof number and Modified Grashof number, the velocity profiles u are plotted in Figure-2 and Figure-3. The Grashof number (Gr) signifies the relative effect of the thermal buoyancy force to the viscous hydrodynamic force in the boundary layer. As expected, it is observed that there is a rise in the velocity due to the enhancement of thermal buoyancy force. Also, as Gr increases, the peak values of the velocity increases rapidly near the porous plate and then decays smoothly to the free stream velocity. The Modified Grashof number (Gc) defines the ratio of the species buoyancy force to the viscous hydrodynamic force. As expected, the fluid velocity increases and the peak value is more distinctive due to increase in the species buoyancy force. The velocity distribution attains a distinctive maximum value in the vicinity of the plate and then decreases properly to approach the free stream value. It is noticed that the velocity increases with increasing values of Modified Grashof number (Gc). Figure-4 illustrates the velocity profiles for different values of Prandtl number $\Pr$. The numerical results show that the effect of increasing values of Prandtl number result in decreasing velocity. The nature of velocity profiles in presence of foreign species such as Hydrogen (Sc = 0.22), Helium (Sc = 0.22), Oxygen (Sc = 0.60) and Water vapour (Sc = 0.66) are shown in Figure-5.

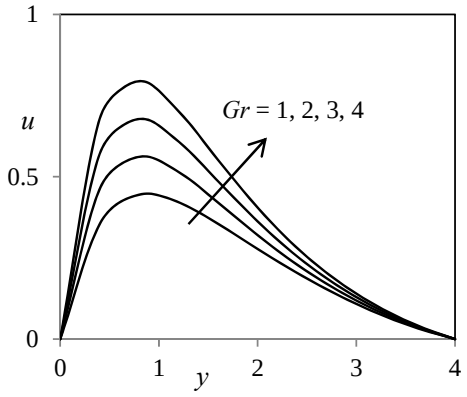

Figure-2. Velocity profiles for different values of *Gr.*

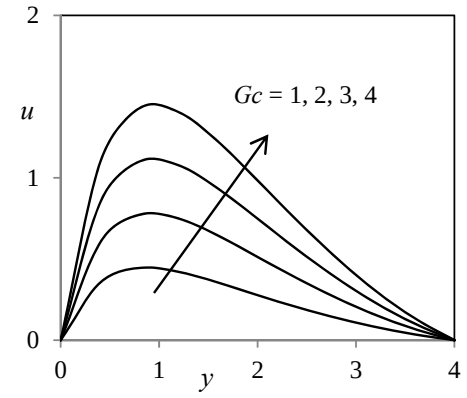

Figure-3. Velocity profiles for different values of *Gc.*

The flow field suffers a decrease in primary velocity at all points in presence of heavier diffusing species. The effect of the magnetic field parameter M is shown in Figure-6 in case of cooling of the plate. It is observed that the velocity of the fluid decreases with the increase of the magnetic field parameter values. The decrease in the velocity as the Hartmann number M increases is because the presence of a magnetic field in an electrically conducting fluid introduces a force called the Lorentz force, which acts against the flow if the magnetic field is applied in the normal direction, as in the present study. This resistive force slows down the fluid velocity component as shown in Figure-6. The variations of velocity distribution with y for different values of the Dufour number (Du) and Soret number (Sr) are shown in Figure-7 and Figure-11. It can be clearly seen that the velocity distribution in the boundary layer increases with the Dufour and Soret numbers.

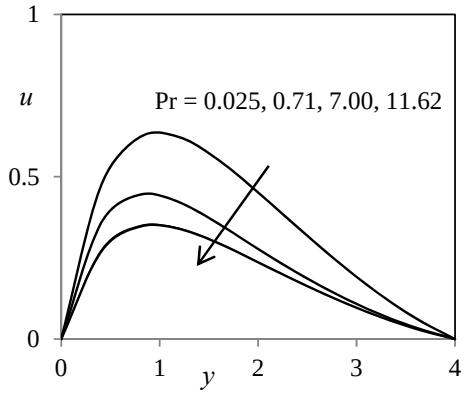

Figure-4. Velocity profiles for different values of Pr.

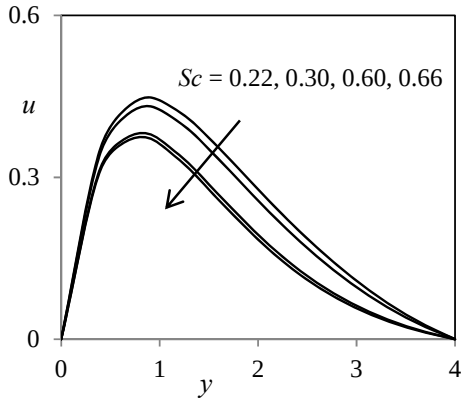

Figure-5. Velocity profiles for different values of *Sc*.

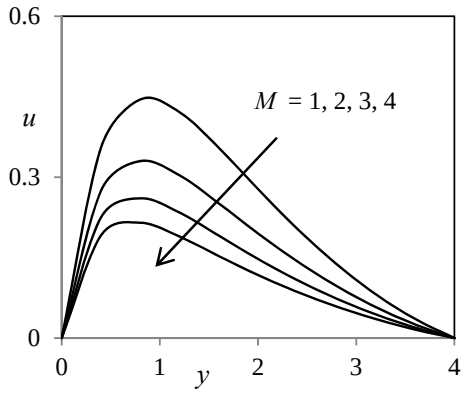

Figure-6. Velocity profiles for different values of *M*.

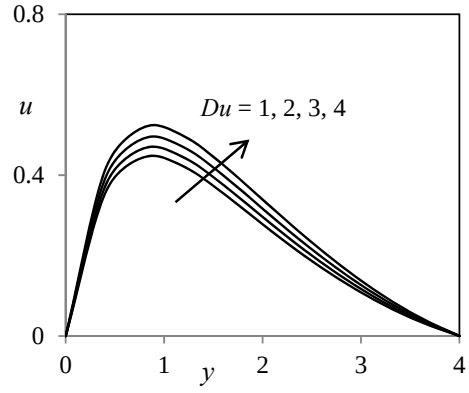

Figure-7. Velocity profiles for different values of *Du*.

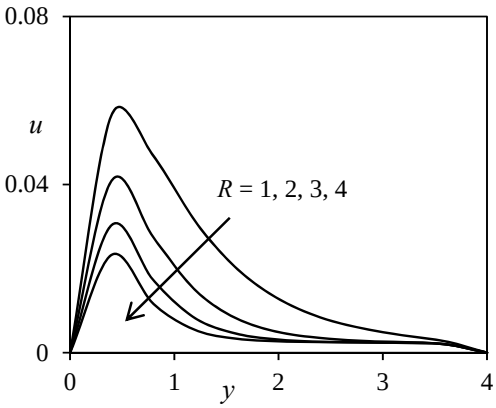

Figure-8. Velocity profiles for different values of *R*.

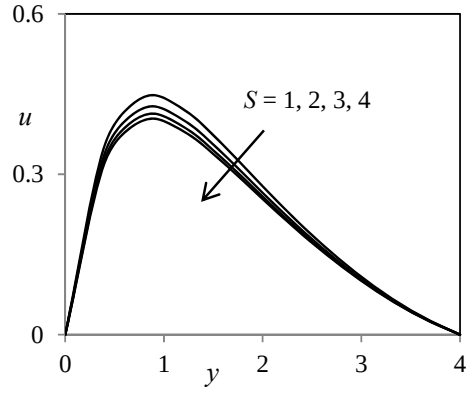

Figure-9. Velocity profiles for different values of *S*.

The effect of the thermal radiation parameter R on the primary velocity and temperature profiles in the boundary layer are illustrated in Figure-8 and Figure-15 respectively. Increasing the thermal radiation parameter R produces significant increase in the thermal condition

of the fluid and its thermal boundary layer. This increase in the fluid temperature induces more flow in the boundary layer causing the velocity of the fluid there to increase. Figure-9 and Figure-14 has been plotted to depict the variation of velocity and temperature profiles against y for different values of heat source parameter S by fixing other physical parameters. From this Graph we observe that velocity and temperature decrease with increase in the heat source parameter S because when heat is absorbed, the buoyancy force decreases the temperature profiles. Figure-10 shows the effects of Darcy number χ on the velocity profiles for cooling as well as heating of the plate. For a cooling plate fluid velocity increases, whereas for a heating plate it decreases with increase of χ. Darcy number is the measurement of the porosity of the medium. As the porosity of the medium increases, the value of χ increases. For large porosity of the medium fluid gets more space to flow as a consequence its velocity increases. Figure-12 illustrates the temperature profiles for different values of Prandtl number $\Pr$. It is observed that the temperature decrease as an increasing the Prandtl number. The reason is that smaller values of Pr are equivalent to increase in the thermal conductivity of the fluid and therefore heat is able to diffuse away from the heated surface more rapidly for higher values of Pr. Hence in the case of smaller Prandtl number the thermal boundary layer is thicker and the rate of heat transfer is reduced. The Dufour number (Du) does not enter directly into the momentum and mass equations. Thus the effect of Dufour number on velocity and mass profiles is not apparent.

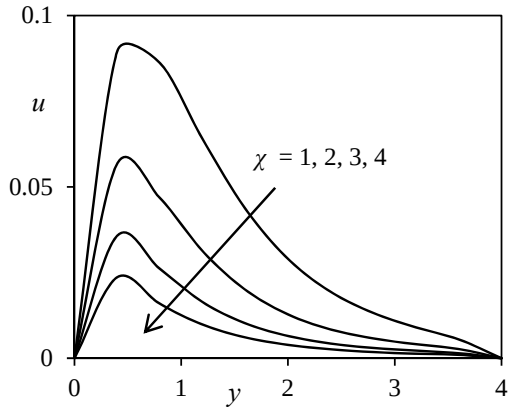

Figure-10. Velocity profiles for different values of χ.

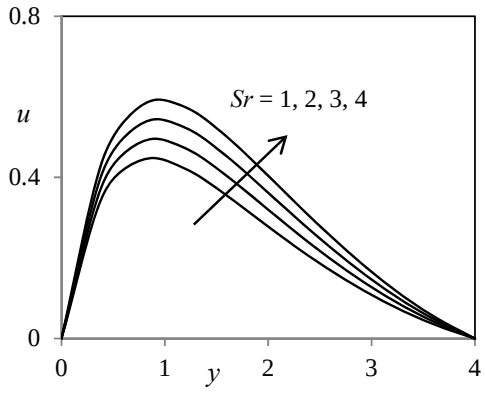

Figure-11. Velocity profiles for different values of *S.*

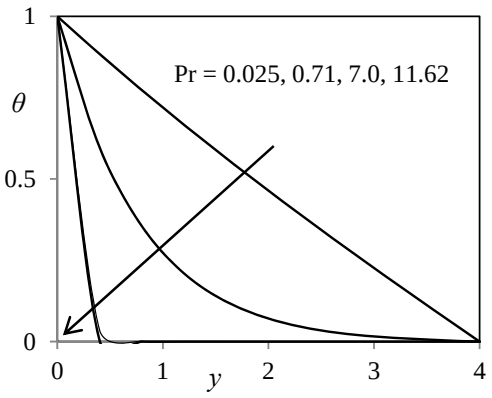

Figure-12. Temperature profiles for different values of Pr.

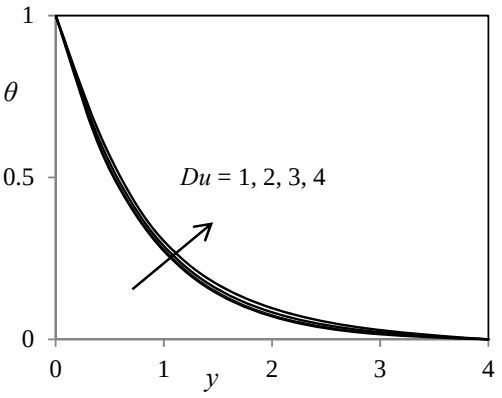

Figure-13. Temperature profiles for different values of *Du.*

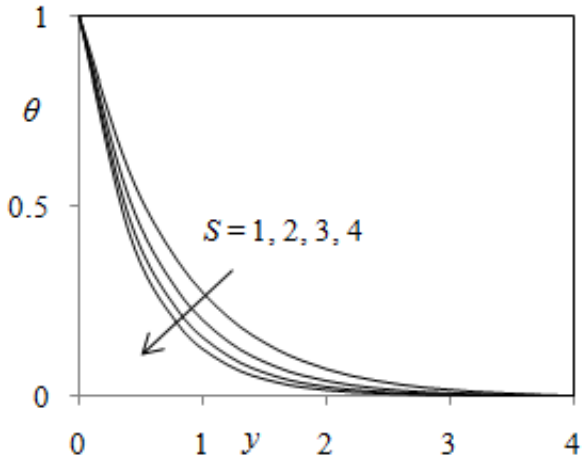

Figure-14. Temperature profiles for different values of *S*.

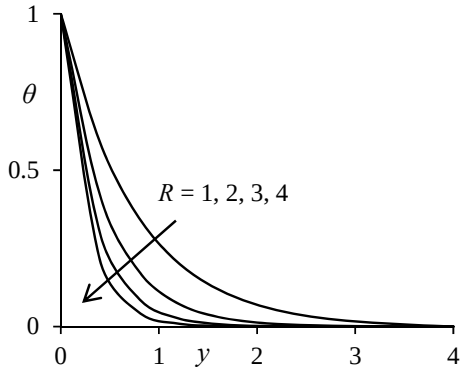

Figure-15. Temperature profiles for different values of *R*.

Figure-13 shows the variation of temperature profiles for different values of Du. The parameter Du has marked effects on the temperature profiles. It is observed that the temperature profiles increase with the increasing values of Du. It is also observed from this figure that when Du = 1.0, that is, when the ratio between temperature and concentration gradient is very small the temperature profile shows its usual trend of gradual decay. As Dufour number Du becomes large the profiles overshoot the uniform temperature close to the boundary. The effects of Schmidt number (Sc) and Soret number (Sr) on the concentration field are presented in Figure-16 and Figure-17.

Table-1. Variation of numerical values of Skin-friction (τ) for different values of Gr, Gc, Sc, Pr, M, χ, Sr, Du, S and R.

Gr	*Gc*	Pr	*Sc*	*M*	χ	*Sr*	*Du*	*S*	*R*	τ
1.0	1.0	0.71	0.22	2.0	1.0	1.0	1.0	1.0	1.0	3.26981158
2.0	1.0	0.71	0.22	2.0	1.0	1.0	1.0	1.0	1.0	4.10593294
1.0	2.0	0.71	0.22	2.0	1.0	1.0	1.0	1.0	1.0	4.58411658
1.0	1.0	7.00	0.22	2.0	1.0	1.0	1.0	1.0	1.0	2.85204877
1.0	1.0	0.71	0.60	2.0	1.0	1.0	1.0	1.0	1.0	2.88523694
1.0	1.0	0.71	0.22	4.0	1.0	1.0	1.0	1.0	1.0	2.95431478
1.0	1.0	0.71	0.22	2.0	2.0	1.0	1.0	1.0	1.0	3.01140566
1.0	1.0	0.71	0.22	2.0	1.0	2.0	1.0	1.0	1.0	3.36951587
1.0	1.0	0.71	0.22	2.0	1.0	1.0	2.0	1.0	1.0	3.30683951
1.0	1.0	0.71	0.22	2.0	1.0	1.0	1.0	2.0	2.0	2.99852642
1.0	1.0	0.71	0.22	2.0	1.0	1.0	1.0	1.0	2.0	2.85461148

Table-2. Variation of Nusselt number (Nu) for different values of Pr, Du, S and R.

Pr	Du	S	R	Nu
0.71	**1.0**	**1.0**	**1.0**	**1.97641695**
7.00	1.0	1.0	1.0	1.75303026
0.71	2.0	1.0	1.0	2.05714089
0.71	1.0	2.0	1.0	1.69580334
0.71	1.0	1.0	2.0	1.86821198

Table-3. Variation of Sherwood number (Sh) for different values of Sc and Sr.

Sc	Sr	Sh
0.22	**1.0**	**1.69498587**
0.30	1.0	1.52094930
0.22	2.0	1.78854463

Table-4. Comparison of present Skin-friction results (τ) with the Skin-friction results (τ^*) obtained by Israel-Cookey *et al.* (2003) for different values of Gr, Pr, M, χ and R.

Gr	Pr	M	R	χ	τ	τ^*
1.0	0.71	2.0	1.0	1.0	2.23596954	2.23220095
2.0	0.71	2.0	1.0	1.0	3.25848291	3.25543954
1.0	7.00	2.0	1.0	1.0	1.21697635	1.21580687
1.0	0.71	4.0	1.0	1.0	1.20579208	1.20141692
1.0	0.71	2.0	2.0	1.0	1.98874481	1.98365881
1.0	0.71	2.0	1.0	2.0	1.85366197	1.85053396

Figure-16 shows the concentration field due to variation in Schmidt number (Sc) for the gasses Hydrogen, Helium, Water-vapour, Oxygen and Ammonia. It is observed that concentration field is steadily for Hydrogen and falls rapidly for Oxygen and Ammonia in comparison to water-vapour. Thus Hydrogen can be used for maintaining effective concentration field and Water-vapour can be used for maintaining normal concentration field. In Figure-17, it is observed that an increase in the Soret number (Sr) leads to increase in the concentration field. Table-1 shows the variation of different values Gr, Gc, Pr, Sc, M, χ, S, Sr, Du, and R on Skin-friction (τ). From this table it is concluded that the Skin-friction (τ) increases as the values of Gr, Gc, Sr and Du increase and this behavior is found just reverse with the increase of Pr, Sc, M, χ, S and R. Table-2 shows the variation of Nusselt number (Nu) different values of Pr, Du, S and R. From this Table it is concluded that the Nusselt number (Nu) increases as the value of Du increases and this behavior is found just reverse with the increase of Pr, S and R. Table-3 shows the variation of Sherwood number (Sh) different values of Sc and Sr. From this table it is concluded that Sherwood number (Sh) increase as the value of Sr increases and this behavior is found just reverse with the increase of Sc. In order to ascertain the accuracy of the numerical results, the present skin-friction (τ) results are compared with the previous skin-friction (τ^*) results of Israel-Cookey *et al.* (2003) in table-4. They are found to be in an excellent agreement.

CONCLUSIONS

In conclusion therefore, the flow of an unsteady MHD free convection past an infinite heated vertical plate

in a porous medium under the simultaneous effects of thermal-diffusion, diffusion-thermo, radiation and heat source is affected by the material parameters. The governing equations are approximated to a system of linear partial differential equations by using Galerkin finite element method. The results are presented graphically and we can conclude that the flow field and the quantities of physical interest are significantly influenced by these parameters.

a) The velocity increases as Grashof number Gr, Modified Grashof number Gc, Dufour number Du and Soret number Sr increases. However, the velocity was found to decreases as the Hartmann number M, Prandtl number $\Pr$, Schmidt number Sc, Thermal radiation parameter R, Heat source parameter S and Darcy parameter χ are increases.

b) The fluid temperature was found to decreases as the thermal radiation parameter R, Heat source parameter S and Prandtl number $\Pr$ are increases and found to increase as Dufour number Du increases.

c) The fluid concentration was found to decreases as the Schmidt number Sc and increases as the Soret number Sr increases.

d) From Table-1, it is concluded that the Skin-friction (τ) increases with the increasing values of Gr, Gc, Sr and Du and this behavior is found just reverse with the increasing of $\Pr$, Sc, M, χ, S and R.

e) From table-2, it is concluded that the Nusselt number (Nu) increases with the increasing values of Du and this behavior is found just reverse with the increasing of $\Pr$, S and R.

f) From table-3, it is concluded that the Sherwood number (Sh) increases with the increasing values of Sr and this behavior is found just reverse with the increasing of Sc.

g) On comparing the Skin-friction (τ) results with the Skin-friction (τ^*) results of Israel-Cookey *et al.* (2003) in Table-4. It can be seen that they agree very well.

Nomenclature

A	Small positive parameter
T_w'	Wall temperature
T_∞'	Reference temperature
U'	Dimensional free stream velocity
t'	Dimensional time
g	Acceleration due to gravity
w_0'	Dimensional suction velocity
(u', v', w')	Dimensional velocity components
(x', y')	Dimensional Cartesian coordinates
$H_0'^2$	Constant transverse magnetic field
k	Dimensional porosity parameter
c_p	Specific heat capacity
c_s	Concentration susceptibility
M^2	Non-dimensional Hartmann number
$\Pr$	Prandtl number
Gr	Grashof number
Gc	Modified Grashof number
Sc	Schmidt number
Sr	Soret number
Du	Dufour number
D	Chemical diffusivity
D_m	Molecular diffusivity
k_T	Mean absorption coefficient
C'	Concentration
C	Dimensionless concentration
C_w'	Concentration near the plate
C_∞'	Concentration in the fluid far away from the plate
R^2	Radiation parameter
U_0	Mean velocity of $U'(t')$
$q_{z'}'$	Radiative heat flux
B	Planck's function
S	Heat source

Greek symbols

ε	Small positive parameter
β	Coefficient of Volume expansion

β^*	Volumetric Coefficient of Expansion with Concentration
v	Kinematic viscosity
σ_C	Electrical conductivity
μ	Permeability
ρ	Fluid density
ω'	Dimensional free stream frequency of oscillation
k	Thermal conductivity
α^2	Absorption coefficient
χ^2	Darcy number
δ	Radiation absorption coefficient

REFERENCES

Rajput US and Sahu PK. 2011. Transient free convection MHD flow between two long vertical parallel porous plates with variable temperature and mass diffusion. ARPN Journal of Engineering and Applied Sciences. 6(8): 79-86.

Anand Rao J and Srinivasa Raju R. 2010. Applied magnetic field on transient free convective flow of an incompressible viscous dissipative fluid in a vertical channel. Journal of Energy, Heat and Mass Transfer. 32: 265-277

El-Amin MF. 2001. Magnetohydrodynamic free convection and mass transfer flow in micropolar fluid with constant suction. Journal of Magnetism and Magnetic Materials. 234(3): 567-574.

Chaudhary RC and Sharma BK. 2006. Combined heat and mass transfer by laminar mixed convection flow from a vertical surface with induced magnetic field. Journal of Applied Physics. 99(3): 34901-34910.

Sharma BK and Chaudhary RC. 2008. Hydromagnetic unsteady mixed convection and mass transfer flow past a vertical porous plate immersed in a porous medium with hall effect. Engineering Transactions. 56(1): 3-23

Kandasamy R, Periasamy K and Prashu Sivagnana KK. 2005. Effects of chemical reaction, heat and mass transfer along wedge with heat source and concentration in the presence of suction or injection. International Journal of Heat and Mass transfer. 48(7): 1388-1394.

Kandasamy R, Hashim I, Muhaimin and Ruhaila. 2007. Effects of variable viscosity. Heat and mass transfer on nonlinear mixed convection flow over a porous wedge with heat radiation in the presence of homogenous chemical reaction. ARPN Journal of Engineering and Applied Sciences. 2(5): 44-53

Rajesh V and Vijaya Kumar Varma S. 2009. Radiation and mass transfer effects on MHD free convection flow past an exponentially accelerated vertical plate with variable temperature. ARPN Journal of Engineering and Applied Sciences. 4(6): 20-26

Srinivasa Rao V and Anand Babu L. 2010. Finite element analysis of radiation and mass transfer flow past semi-infinite moving vertical plate with viscous dissipation. ARPN Journal of Engineering and Applied Sciences. 5(11): 40-46.

Anand Rao J, Sivaiah S and Nuslin Sk. 2012. Radiation effects on an unsteady MHD vertical porous plate in the presence of homogeneous chemical reaction. ARPN Journal of Engineering and Applied Sciences. 7(7): 853-859.

Rajput US and Surendra Kumar. 2012. Radiation effects on MHD flow through porous media past an impulsively started vertical oscillating plate with variable mass diffusion. ARPN Journal of Engineering and Applied Sciences. 7(1): 108-113.

Vijaya Kumar AG, Raveendra Babu K, Reddappa B and Varma SVK. 2013. Effects of chemical reaction and radiation absorption on the unsteady MHD free convective flow past an infinite vertical moving plate with constant heat source. ARPN Journal of Engineering and Applied Sciences. 8(5): 377-385.

Israel-Cookey C, Ogulu A and Omubo-Pepple VB. 2003. Influence of viscous dissipation and radiation on unsteady MHD free convection flow past an infinite heated vertical plate in a porous medium with time-dependent suction. International Journal of Heat and Mass Transfer. 46: 2305-2311.

Mohammad Ali and Mohammad Shah Alam. 2014. Soret and Hall Effect on MHD flow. Heat and mass transfer over a vertical stretching sheet in a porous medium due to heat generation. ARPN Journal of Engineering and Applied Sciences. 9(3): 361-371.

Anand Rao J and Srinivasa Raju R. 2011. The effects of Hall currents. Soret and Dufour on MHD flow and heat transfer along a porous flat plate with mass transfer. Journal of Energy, Heat and Mass Transfer. 33: 351-372.

Postelnicu A. 200 Influence of a magnetic field on heat and mass transfer by natural convection from vertical surfaces in porous media considering Soret and Dufour effects. International Journal of Heat and Mass Transfer. 47(6-7): 1467-1472.

Afify AA. 2009. Similarity solution in MHD effects of thermal-diffusion and diffusion-thermo on free convective heat and mass transfer over a stretching surface considering suction and injection. Communications Nonlinear Science and Numerical Simulation. 14: 2202-2214.

Alam S, Rahman MM, Maleque A and Ferdows M. 2006. Dufour and Soret effects on steady MHD combined free forced convective and mass transfer flow past a semi infinite vertical plate. Thammasat International Journal Science and Technology. 11(2).

Mansour MA, El-Anssary NF and Aly AM. 2008. Effects of chemical reaction and thermal stratification on MHD free convective heat and mass transfer over a vertical stretching surface embedded in a porous media considering Soret and Dufour numbers. Chemical Engineering Journal. 145(2): 340-345.

Osalusi, Side E and Harris R. 2008. Thermal-diffusion and diffusion-thermo effects on combined heat and mass transfer of steady MHD convective and slip flow due to a rotating disk with viscous dissipation and Ohmic heating. International Communications in Heat and Mass Transfer. 35: 908-915.

Srinivasa Raju R, Sudhakar K and Rangamma M. 2013. The effects of thermal radiation and Heat source on an unsteady MHD free convection flow past an infinite vertical plate with thermal-diffusion and diffusion-thermo, Journal of Institution of Engineers (India): Series C. 94(2): 175-186.

Cogley AC, Vincenti WG and Gilles SE. 1968. Differential approximation for radiative transfer in a Non-grey gas near equilibrium. American Institute of Aeronautics and Astronautics. 6: 551-553.